Estimates of tree root water uptake from soil moisture profile dynamics

Conrad Jackisch[1,2], Samuel Knoblauch[1,3], Theresa Blume[4], Erwin Zehe[1], and Sibylle K. Hassler[1]

[1]Karlsruhe Institute of Technology (KIT), Institute of Water and River Basin Management, Chair of Hydrology, Kaiserstr. 12, 76131 Karlsruhe, Germany.
[2]Technische Universität Braunschweig, Institute of Geoecology, Dept. Landscape Ecology and Environmental Systems Analysis, Langer Kamp 19c, 38106 Braunschweig, Germany.
[3]University of Greifswald, Dept. of Biology, Friedrich-Ludwig-Jahn-Str. 15, 17489 Greifswald, Germany.
[4]Helmholtz Centre Potsdam, GFZ German Research Centre for Geosciences, Section Hydrology, Potsdam, Germany.

Correspondence: Conrad Jackisch (c.jackisch@tu-braunschweig.de)

Abstract. Root water uptake (RWU) as one important process in the terrestrial water cycle can help to better understand the interactions in the soil water plant system. We conducted a field study monitoring soil moisture profiles in the rhizosphere of beech trees at two sites with different soil conditions. We infer RWU from step-shaped, diurnal changes in soil moisture. While this approach is a feasible, easily implemented method during wet and moderate conditions, limitations were identified during

5 drier states and for more heterogeneous soil settings. A comparison with time series of xylem sap velocity reveals that RWU and sap flow are complementary measures of the transpiration process. The high correlation between the sap flow time series of the two sites, but lower correlation between the RWU time series, suggests that the trees adapt RWU to soil heterogeneity and site differences.

10 **1 Introduction**

Evapotranspiration (ET) is a key water and energy flux in ecosystems. Although ET amounts globally to 60% of total precipitation in terrestrial systems (Oki and Kanae, 2006) and transpiration is claimed to dominate the terrestrial water cycle (Jasechko et al., 2013), it remains one of the most challenging fluxes to observe and understand (Wulfmeyer et al., 2018). ET describes the transport of water from the soil towards the atmosphere, influenced by soil characteristics determining water supply, at-

15 mospheric conditions acting as driving gradient and land use and vegetation characteristics controlling the transport. While evaporation is addressed in experiments and models (Shuttleworth, 2007; Or et al., 2013) and can be modelled reasonably well, ET dynamics at sub-daily resolution is still challenging (Renner et al., 2019) – even over grasslands.

Transpiration of vascular plants, which optimise their water transport to respiration (Schymanski et al., 2009), adds complexity in the ecohydrological and thermodynamical system. Moreover, the controls of transpiration are not static in a forest

20 stand (Renner et al., 2016; Dubbert and Werner, 2019). Additionally, plants can store water to buffer intermediate stresses

(Gao et al., 2014). Studies on plant transpiration frequently focus on stomatal control (Schymanski and Or, 2017) and theories on leaf-related dynamics and the transpiration loss function (Sperry and Love, 2015). To estimate transpiration of individual trees, sap flow (SF) measurements are widely used (e.g. Nadezhdina et al., 2010; Poyatos et al., 2016). However, a series of approximations and assumptions is needed to convert the sap velocity values in the xylem to the water transport of a whole tree
5 or even to stands.

For root water uptake (RWU) as an indicator of water supply for the plant and possibly an estimate of transpiration, comparably few studies and measurement standards exist. For small plants, lysimeters are a means to infer the overall effect of plants on ET (e.g. Gebler et al., 2015). More details about the shape of the rhizosphere can be revealed with tomographic analyses (e.g. Kuhlmann et al., 2012; Pohlmeier et al., 2017), but not necessarily about the dynamic RWU process in the rhizosphere. At
10 larger scale and for larger plants, changes of groundwater levels (e.g. Maxwell and Condon, 2016; Blume et al., 2018), isotope signatures of water (e.g. Dubbert and Werner, 2019) and carbon (e.g. Vidal et al., 2018), and sap flow measurements in the roots have been employed (e.g. Burgess et al., 2000). To understand RWU, a series of approaches to measure (e.g. Mary et al., 2016) and simulate (e.g. Pagès et al., 2004; Javaux et al., 2008) the root architecture and its interaction with soil hydrology have been developed. Among these representation through resistance terms (e.g. Couvreur et al., 2012) or thermodynamic optimisation
15 based on the assumption that the plant minimises physical work during root water uptake (Hildebrandt et al., 2016) have been proposed. It is known that RWU responds to soil water conditions (Cai et al., 2018) and thus soil structure. Additionally, studies found that roots and soil structure co-evolve (Carminati et al., 2012) and that roots can actively modify the soil properties by mucilage (Carminati et al., 2016; Kroener et al., 2018).

So far, only few examples for in situ observations of tree RWU dynamics exist (e.g. Rodríguez-Robles et al., 2017; Leuschner
20 et al., 2004). From a soil perspective, the complex effect of RWU can be observed as a decrease of soil water content during active water transport through plants (Feddes and van Dam, 2005; Guderle and Hildebrandt, 2015), but spatially distributed measurements of soil moisture dynamics at relevant scales are just emerging (Klenk et al., 2015; Allroggen et al., 2017; Boaga et al., 2013). However, there has not been much research on how well this diurnal decrease reflects the water transport into and within trees. A change of soil moisture is not necessarily RWU, SF and eventually transpiration. It can also be
25 caused by hydraulic redistribution (Burgess et al., 1998). Hence, following the notion of spatially distributed monitoring of soil water dynamics to reveal function (Jackisch et al., 2017), the spatio-temporal dynamics of soil-moisture-derived RWU and its correlation to SF might be key to develop means to more holistic observations (York et al., 2016) of forest water dynamics and its spatial patterns. Furthermore, spatially distributed monitoring of both RWU from soil moisture and SF could help to elucidate differences between the influence of the geological and pedological settings on water supply to transpiration and the
30 influence of the plants themselves and their adaptations in root systems, dynamic sourcing of water (Nadezhdina et al., 2010) and transpiration efficiency.

The aim of this study is to evaluate the potential and limitations of the diurnal decrease of rhizosphere soil moisture measurements as an estimate for RWU (Guderle and Hildebrandt, 2015; Guderle et al., 2018) in ecohydrological field studies, focusing on forest systems. We test the following hypotheses:

35 **1.** Daily RWU can be robustly derived from records of diurnal soil moisture dynamics.

2. The dynamics in derived RWU is consistently related to dynamics in SF.

3. The effect of soil and site characteristics on RWU is mainly driven by the tension gradient between ET demand and soil matric potential.

For this analysis we develop and assess an automated approach to derive RWU estimates from soil moisture profile mea-
surements. Moreover, we compare the RWU dynamics to sap flow measurements. In order to compare volumetric fluxes, we
apply an estimate for the active sapwood cross-section. We examine the relation of RWU and SF in two beech stands of dif-
ferent geological and pedological setting but with very similar weather, climate and topography in a catchment in western
Luxembourg.

2 Field sites and monitoring methods

In the vegetation period of 2017, we selected and instrumented two sites in mixed beech stands (*Fagus sylvatica*) in contrasting
geological settings, one on loamy sand in a sandstone basin (sandy site) and another on loamy regosol on periglacial coverbeds
of the slate Ardenne Massif (slate site, Fig. 1). Both sites are located in the Attert experimental watershed (Hassler et al., 2018).
The climate is temperate semi-oceanic, mean annual rainfall is 845 mm (Pfister et al., 2014) and mean monthly temperatures
range between 0°C in January and 17°C in July (Wrede et al., 2015).

2.1 Soil hydraulic characteristics of the sites

The sandy site is located in the Huewelerbach subbasin which is characterised by deep, homogeneous sandy soils and deep
groundwater-driven hydrology. The second site on regosol of the slate Ardenne Massif is located in the northern part of the
Colpach subbasin. There, the hydrological regime is dominated by flashy reaction through macroporous soils and fill-and-spill
mechanisms of subsurface pools on the jointed bedrock (Jackisch, 2015; Loritz et al., 2017).

Soil water retention properties of these soils were assessed in a previous study using the free evaporation method of the
HYPROP apparatus and the chilled mirror method in the WP4C (both Meter AG) with $250\,\mathrm{ml}$ undisturbed soil samples from
the sites (Jackisch, 2015). Following this method, the matric potential is divided into bins (0.05 pF). All retention data of the
reference soil samples is bin-wise averaged to form the basis for the fitting of a retention curve (Figure 2, parameters in table
A1). We have aggregated the results of 44 and 41 soil samples in the subbasins of the sand and slate site for a more robust
representation (as discussed by Loritz et al., 2017).

2.2 Monitoring techniques

Soil moisture was monitored using a sequence of TDR tube probes (Pico Profile T3PN, Imko GmbH), which allow for in-
stallation with minimal disturbance using an acrylic glass access liner (diameter $48\,\mathrm{mm}$). The liner tube was installed in the
rhizosphere of the trees without any excavation using a percussion drill (about $0.5\,\mathrm{m}$ from the stem). For optimal contact of
the liner with the surrounding soil, the drill diameter was $40\,\mathrm{mm}$ and the tube was installed more than one year prior to the
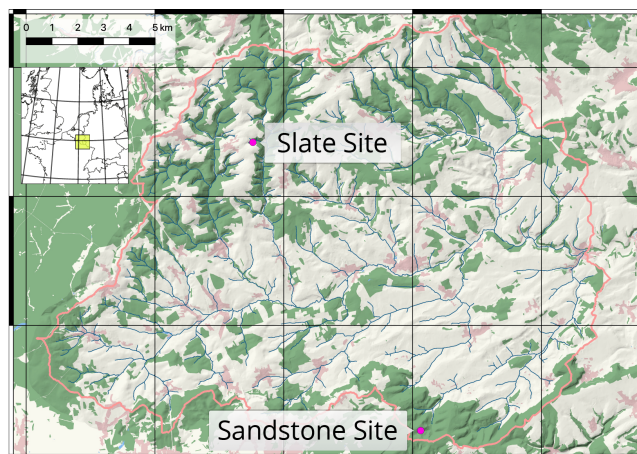
Figure 1. Attert experimental basin, Western Luxembourg. Locations of the two reference sites. Basemap: Landcover from OpenStreetMap contributors. Shading and river network calculated with a combined DEM of the administrations of Luxembourg and Wallonie.
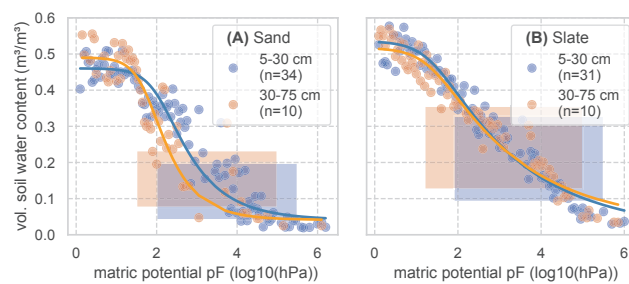

Figure 2. Soil water retention curves for two soil layers at both experimental sites. To derive the retention curves, the matric potential is divided into bins of 0.05 pF. Measured soil moisture values of all samples and at tensions that fall into each bin are averaged and displayed as dots. The retention curve is fitted to these points. The resulting van Genuchten parameters are given in table A1. The number of soil samples that form the basis for the retention curves is given as n. The shaded areas mark the range of soil moisture values we observed with the TDR probes in this study.

Biogeosciences
Discussions
Open Access
EGU

recorded data set. Each TDR probe segment integrates the soil moisture measurement over its length of $0.2\,\mathrm{m}$. The signal penetrates the soil about $0.05\,\mathrm{m}$ which results in an integral volume of approx. $0.001\,\mathrm{m}^3$. The probes are stacked directly on top of each other, permitting spatially continuous monitoring over the soil moisture profile.

At the sandy site, we were able to install a profile with a sequence of 12 probes reaching a depth of $2.4\,\mathrm{m}$. At the slate site,
5 percussion drilling was inhibited by the weathered bedrock. There, we installed a profile with a sequence of 9 probes reaching a depth of $1.8\,\mathrm{m}$.

Sap velocities were monitored in four beech trees in the direct vicinity of the soil moisture profile (as part of the CAOS research unit). At the sandy site, the reference sap velocity time series could be obtained from the exact tree where the TDR sensors were installed. It had a diameter at breast height (DBH) of $64\,\mathrm{cm}$. At the slate site, the sap velocity sensor of the intended
10 tree failed 3 weeks after leaf out. There, we refer to a neighbouring beech tree with a DBH of $48\,\mathrm{cm}$ about $9\,\mathrm{m}$ from the TDR measurements (see Appendix A for details). The sap flow sensors (East30 Sensors) are based on the heat ratio method and measure simultaneously at 5, 18 and $30\,\mathrm{mm}$ depth within the sapwood. Installation and calculation of sap velocities followed the description in Hassler et al. (2018). The sensors were installed before leaf out of the vegetation period. As further reference for the drivers of temporal dynamics in soil moisture and sap velocity we use solar radiation records (Apogee Pyranometer
15 SP110) and corrected radar stand precipitation at canopy level (data from DWD (Deutscher Wetterdienst, Germany), ASTA (Administration des Services techniques de l'agriculture, Luxembourg) and KNMI (Koninklijk Nederlands Meteorologisch Instituut, Netherlands) combined after Neuper and Ehret, 2019).

3   Inferring daily RWU from change in soil moisture

On days with very little vertical soil water movement, step-like dynamics of soil moisture are observed (Guderle and Hilde-
20 brandt, 2015). These steps coincide and highly correlate with the observed sap flow dynamics. In an exemplary three-day time series in Fig. 3 the correlation between changes in soil moisture and sap velocity give a Spearman rank correlation (r_s) of 0.87 and when linearly scaled to the same mean a Kling-Gupta-Efficency (KGE, which is sensitive to curve fitting and its absolute values) of 0.64. Especially on June 15 the coherence between solar radiation, sap velocity and change in soil moisture becomes very obvious, when intermittent cloudiness lets radiation and sap velocity drop in the afternoon. During the same period the
25 decline of soil moisture is halted, too. Furthermore, one can see that the signal of sap velocity follows the solar radiation with a slight time lag. Change in soil moisture follows the same pattern. When we can exclude percolation and pedophysical soil water redistribution as main drivers of soil moisture change, we may attribute these observed steps in the rhizosphere soil water content to RWU.

3.1   RWU calculation

30 Based on the idea of Guderle and Hildebrandt (2015) and Blume et al. (2016), we developed an evaluation algorithm for the observed soil moisture dynamics within the tree rhizosphere to identify the characteristic declines and to extract daily RWU from the measured soil water changes (Fig. 4).
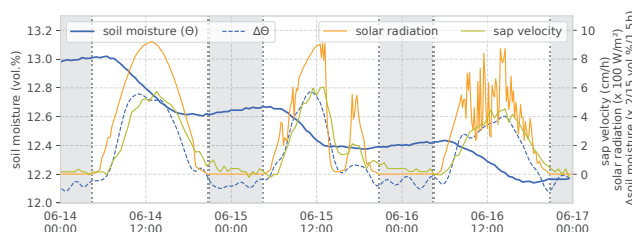
Figure 3. Example of observed solar radiation, sap velocity and soil moisture during three days of the vegetation period. The example is from the sandy site dataset, soil moisture values are in 0.7 m depth. The change in soil moisture compares with sap velocity with $r_s = 0.87$ and when linearly scaled with KGE=0.64.
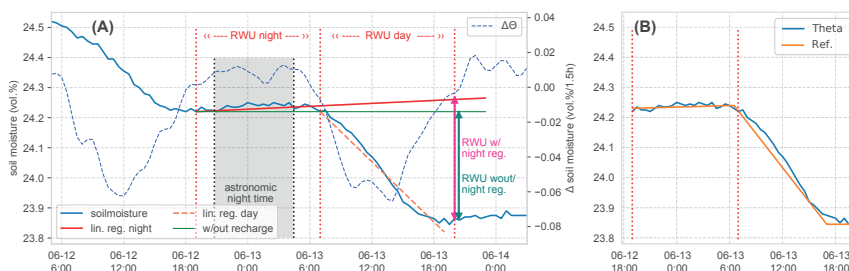

Figure 4. A) Calculation of root water uptake from soil moisture change of one day in one soil layer. B) Comparison to artificial reference step.

First, the inflection points of the time series are identified (Fig. 4A vertical dashed red lines). These points are i) the beginning of a decline of soil moisture after sunrise and ii) the end of this decline near sunset. The astronomic reference times have been calculated with the *Astral* package (Kennedy, 2019) using the geographic positions of the sites. Our algorithm scans for the first soil moisture change of $\geq 0 \, \text{vol} \, \% \, \text{h}^{-1}$ in a window starting five hours before sunset and identifies this as the beginning

5   of the night. The next decrease below $-0.02 \, \text{vol} \, \% \, \text{h}^{-1}$ is marked as beginning of diurnal RWU. The beginning of the next night is used as final evaluation reference. Because the employed TDR sensors show very little noise, we could avoid strong smoothing of the time series of soil moisture changes between three time steps. However, we applied a 1D Gaussian filter with one standard deviation to the resulting time series before evaluation to make the procedure more robust.

Compliance of the day-to-day soil moisture signal with the hypothesised step shape is evaluated with two control measures:

10   First, we construct a synthetic step interpolating between the observed soil moisture values at two successive sunsets and an artificially increased (by $0.01 \, \text{vol} \, \%$) moisture at $3 \, \text{h}$ past sunrise in between (Fig. 4B). This synthetic reference is compared to the observed time series by calculating the Nash-Sutcliffe-Efficiency (NSE). The NSE is a measure which is very sensitive to deviations from shape features. As second set of criterions, we fit two linear regression models to the night and day phases of the observed time series (Fig. 4A). With the following consistency checks we can evaluate the general step shape of the

15   observed curves (a) and the absence of strong external fluxes dominating changes in soil moisture (b):

a) day slope of soil moisture (a_{day}) is negative (decline in soil moisture during the day) and three times smaller than night slope (general step shape of the curve).

$$min(0, 3a_{\mathrm{night}}) > a_{\mathrm{day}} \tag{1}$$

b) night slope of soil moisture (a_{night}) is $\geq -0.01 \, \mathrm{vol\%}/12\,\mathrm{h}$ (no strong decline in soil moisture during the night, which would
5   indicate percolation or external withdrawal as dominating process) and $< 0.02 \, \mathrm{vol\%}/12\,\mathrm{h}$ (no too strong increase in soil moisture during the night, which would indicate an externally driven input of soil water).

$$\frac{0.02\,\mathrm{vol\%}}{12\,\mathrm{h}} > a_{\mathrm{night}} \geq \frac{-0.01\,\mathrm{vol\%}}{12\,\mathrm{h}} \tag{2}$$

Moreover, the nocturnal regression model is used for extrapolation of any externally driven changes of soil moisture. This change is hypothesised to be soil water exchange or recharge with areas surrounding the rhizosphere layer, as "corrected"
10   reference for the difference calculation (Fig. 4 red line). In the identified steps which meet the given criteria, the change in soil water content over the day is calculated with and without a "correction" term at the beginning of the next night period (Fig. 4 magenta and green vertical arrows).

The developed calculation algorithm is published as python package rootwater under MIT license (Jackisch, 2019).

3.2   Conversion of RWU and sap velocity to flux rates

15   In order to rigorously compare the detected RWU (given in change in soil moisture per time) to the observed sap velocity (given in length per time), we have to derive a sap flow integral from the sap velocity dynamics measured at three points of the sap flow sensor (Fig. 5A). This owes to the facts that i) the sapwood cross-section is radial symmetrically larger with larger reference radius, and ii) the sap velocity in the xylem is unevenly distributed over the sapwood area (Gebauer et al., 2008). Ignoring this can lead to strongly erroneous estimates (Čermák et al., 2004).

20   We assume the two outer measurement points in the sapwood to be representative for the radial area between $0 - 11\,\mathrm{mm}$ and $11\,\mathrm{mm} - 24\,\mathrm{mm}$. Both are the mid points between the sensor positions. The inner sensor is representing a flow field, which has been shown to follow a Weibull distribution (Gebauer et al., 2008) in the active sapwood. To estimate the sap velocity distribution at each time step, we fit the Weibull function with the beech-parameters of Gebauer et al. (2008) to the observed measurements at the mid and inner point via a scaling factor (Fig. 5B). For a correct position reference, the bark thickness is
25   removed after Rössler, Günter (2008). Since Gebauer et al. (2008) reported parameters for the Weibull distribution for different tree species, one should note that the effect of these on the estimate for the flow velocity distribution over the sapwood radius is minor (Fig. 5B, purple dashed line for alternative parameters). As inner end, the 95% percentile is used to mark the transition to the inactive sapwood (Gebauer et al., 2008). The resulting time series is now reporting sap flow in $\mathrm{L\,h^{-1}}$ and is aggregated to daily values.

30   Assuming the measured sap flow fully originates in the soil moisture decrease, we can convert the calculated RWU from change in soil moisture per time to a volumetric flux, too. This is done by linear regression of daily sap flow to the sum of
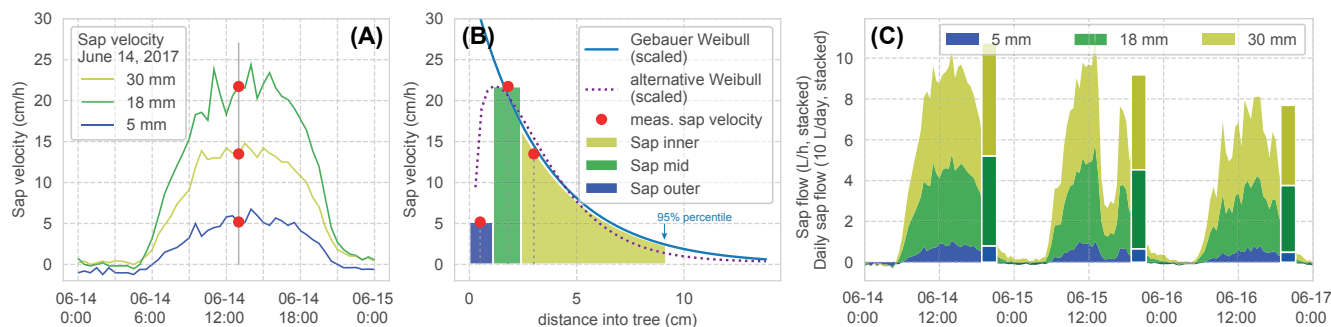
Figure 5. Example for sap flow volume calculation. A) Measured sap velocity on June 14, 2017 with one exemplary sample. B) Application of Weibull distribution of sap velocity in sapwood for the sampled set to derive radial distribution. C) Resulting time series of sap flow and its daily aggregate (bars) after applying the radial sap velocity distribution to a tree with a DBH of $64\,\mathrm{cm}$ for the same days as in Fig. 3.

RWU over the soil profile with assumed zero intercept. The resulting factor is the mean reference area required to supply the observed sap flow. Assuming a circular shape, this yields the mean rhizosphere radius as further evaluation reference for the proposed approach. We acknowledge that the assumption of a closed water balance is probably overly simplified, hence we only consider this approach a rough check-up on general dimensions of the rhizosphere, but we do not interpret the results any

5   further.

3.3   Evaluation of estimated RWU and sap flow

The comparison of derived RWU and SF is done as direct time series analysis and its overall correlation measures. To evaluate the general correlation between the fluxes and sites, we calculate the Spearman rank correlation. As measure being more sensitive to curve shape and absolute volume fluxes, we moreover employ the Kling-Gupta-Efficency (KGE). To account for

10   the non-uniformity of the processes over the vegetation period, the correlation measures are also calculated in a moving window of 21 days. These measures are applied to RWU and SF at each site and for an inter-site comparison.

As reference for the soil hydrological site characteristics, we explore the event water balances of both sites in reaction to a $20\,\mathrm{mm}$ precipitation event in August 2017.

With respect to our third hypothesis, we investigate influences on the observed RWU and sap flow dynamics over the

15   vegetation period on the basis of the soil water state. For this, measured soil moisture is converted into matric potential by applying the measured soil water retention characteristics (Figure 2).

Figure 6. Sap flow (upper part) and RWU estimate (lower part) at two sites. The colour coding of the different depth sources of RWU is complemented with its color strength taken from the NSE evaluation of the step shape evaluation (opaque is high compliance/high NSE).

4 Results

4.1 RWU calculation

Fig. 6 presents time series of sap flow and estimated RWU for both sites. In the top half of each panel stacked daily sap flow and precipitation is given. In the lower half of both panels the stacked RWU estimate from the different soil layers is displayed.

5   At the sandy site, two summer thunderstorms damaged the loggers in the middle of the vegetation period.

The RWU identified from change in soil water content follows the course of sap flow over the year (Fig. 6). It starts with leaf-out and increasing water fluxes through the tree until end of May. In July, both fluxes start to decrease again. In later summer, the RWU signal ceases although the sap flow signal continues at lower rates.

Fig. 6 suggests that the depths of RWU and the magnitude of the sourcing for each depth are not static over the vegetation period. During leaf-out both plots show reactions in deeper layers. Especially at the sandy site, the sourcing from below $1\,\mathrm{m}$ depth can only be found before mid July. But also intermediate horizons appear to disconnect over time. It is interesting to note that the two sites differ mainly in the contributions from the shallow and deeper layers. Uncertainty of the identified RWU is given with less opaque colours for low NSE values of the identified step shape. The transparent colours in summer suggest that the method reaches its limits not only when RWU becomes insignificantly small, but also when soils are dry. Interestingly, the uncertainty of the RWU derivation function is generally smaller at the slate site.

Overall, an answer to our first hypothesis is that a derivation of RWU from changes in soil moisture is possible. However, the time series might be influenced by false-negative results, when the detection failed and resulted in no value. This might be the case at the slate site, when days with similar sap velocity lack a signal from a certain layer (mostly 70 cm end of June and beginning of July). Moreover, some days with reduced sap flow do not show any RWU. Furthermore, quite a number of diurnal RWU sums show uncertainty about the step shape (low NSE and less opaque colour in the plot). Hence, the robustness of the automated detection of the diurnal soil moisture decrease is limited.

4.2 Comparison of seasonal RWU and SF dynamics

With respect to the second hypothesis, despite good general agreement Fig. 6 shows substantial differences of sap flow and the RWU estimate. While we might attribute some of this difference to the limited capabilities of the method, there might also be a difference in RWU and sap flow caused by the different sourcing in the rhizosphere, state of the tree physiology and possible wounding response to the sap flow sensor.

The sites differ strongly in the dynamic pattern of RWU sourcing (Fig. 6). In sand the tree sources RWU from deeper layers during spring and early summer. This deep RWU ceases over the course of the vegetation period although matric potential increases only slightly. Such deep sources were not detected at the slate site. However, we cannot exclude that roots may source water from the weathered bedrock, which would not be detected by the soil moisture sensors.

Looking at the correlation of the RWU estimate and sap flow (Fig. 7), the sandy site presents constantly higher RWU/sap flow ratios during the onset of the growing period compared to summer. However, with an R^2 of 0.91 the correlation of both signals is quite high. At the slate site, the correlation is less well-determined (R^2 of 0.72). Despite the larger scatter, The correlation appears to be influenced by the deviating values in the second half of the vegetation period, which are not included in the sand site data. The correction based on nocturnal changes does not show any substantial effect for the sandy site. However, at the slate site, the method appears to improve the estimates more substantially.

With a working-hypothesis of a closed water balance between SF and RWU, the linear regression also results in an estimate for the mean rhizosphere radius. At the sandy site the cylinder would have a radius of $4.2\,\mathrm{m}$. At the slate site one would
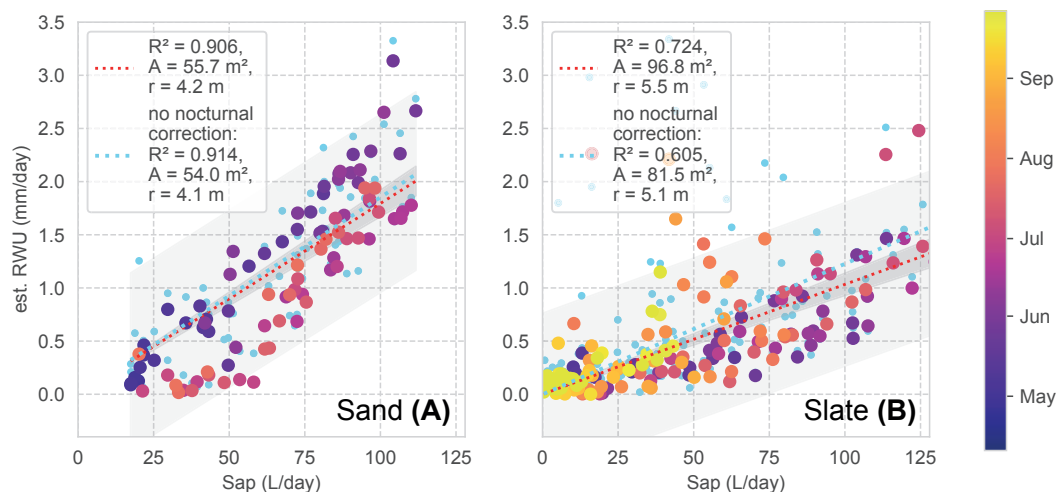
Figure 7. Daily sap flow and cumulated RWU over all soil layers. Colour coding for day of year. Linear regression models given as dashed lines. Light blue dots and regressions are RWU estimates without "nocturnal correction". Grey shades give predicted and observed confidence intervals. The linear regression model is assumed with zero intercept resulting in a scaling factor which is reported as mean area (A) and radius (r) of a cylindrical rhizosphere in the legend.
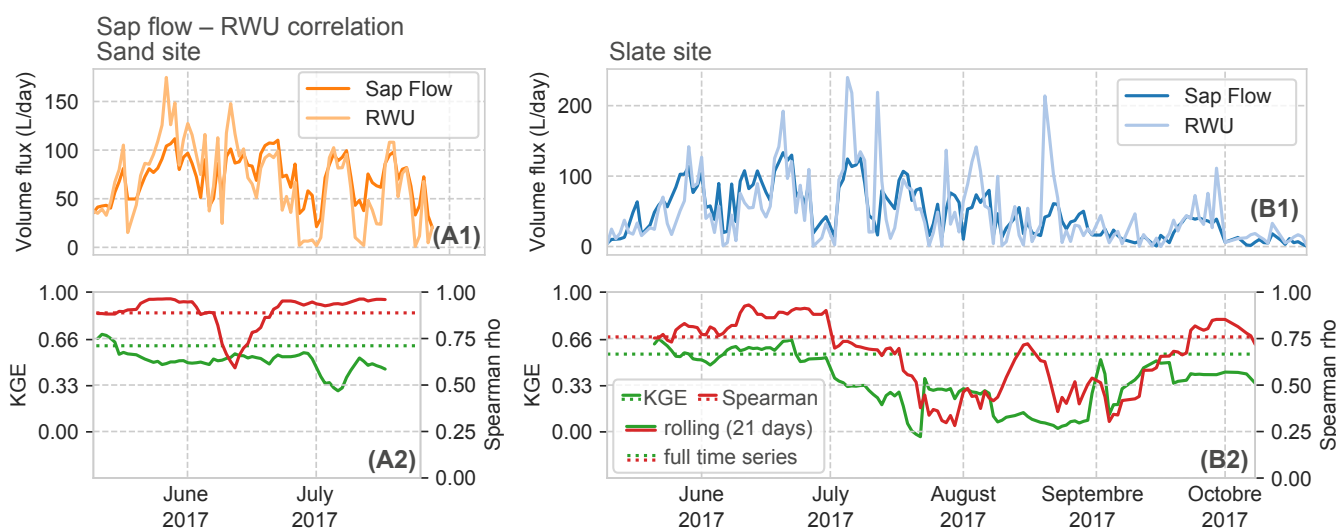

Figure 8. Time series correlation between RWU and sap flow. (A) Sand site, (B) Slate site, A1, B1: Time series plot of calculated daily volume fluxes. A2, B2: Correlation measures.

estimate a radius of $5.5\,\mathrm{m}$. Given the broad assumptions, these values are within a plausible range, corroborating the proposed approach.
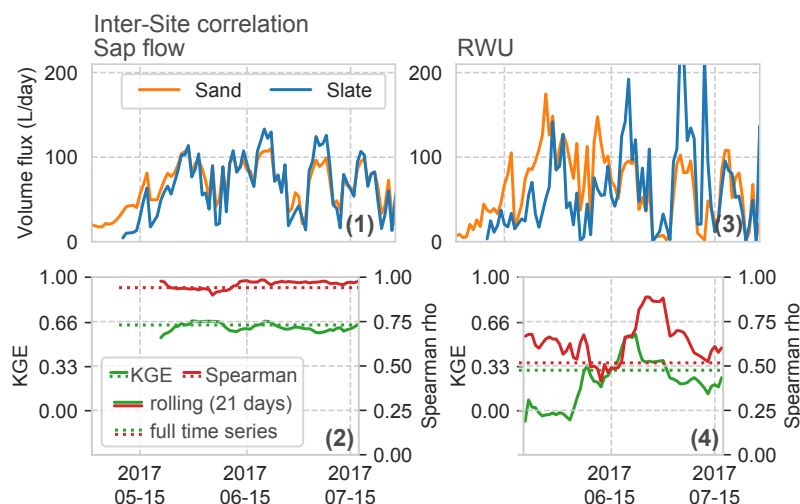
Figure 9. Time series correlation between both sites. 1, 3: Time series of calculated daily volume fluxes. 2, 4: Correlation measures.

The temporal dynamics of the estimate of RWU and observed sap flow correlate quite well with an overall Spearman rank correlation coefficient of 0.89 and 0.76 for sand and slate, respectively (Fig. 8). However, the high initial correlation drops in July. At the sand site, this marks the shift to RWU ranging below SF. At the slate site, no such transition is apparent. The KGE hints to slightly lower correlation of the exact dynamics and flow volumes (0.62 and 0.56 for sand and slate). Both measures corroborate the visual findings in Fig. 6 that the correlation in summer (between July and September) is less convincing. Moreover, these findings point out strong limitations of our working-hypothesis of a closed water balance between RWU and SF.

A comparison between the two sites (Fig. 9) clearly depicts a very high similarity of sap flow (Spearman rho of 0.94 and KGE of 0.64) compared to weaker correlation of RWU (Spearman rho of 0.52 and KGE of 0.3).

So far, the analyses referred to the RWU calculation including the nocturnal correction. The effect of this assumption on the temporally explicit measures is negligible for the sandy site (Spearman improved from 0.85 to 0.89, KGE decreased from 0.66 to 0.62). At the slate site, phases of improved and decreased correlation exist. However, the overall improvement of the Spearman coefficient is from 0.67 to 0.76 points, for KGE from 0.38 to 0.56 when applying the nocturnal correction. Comparing RWU correlation between the two sites, applying the nocturnal correction improves Spearman rho form 0.42 to 0.52. KGE remains almost the same with 0.27 increasing to 0.3.

4.3 Event water balance at both sites

The two sites show contrasting hydrological characteristics. An exemplary event water balance based on the above canopy stand precipitation and the change in soil moisture in the different depth layers is given in Figure 10. While both sites show about 30% of the event water being stored in the soil after five days, the reaction of the soil profiles is very different between
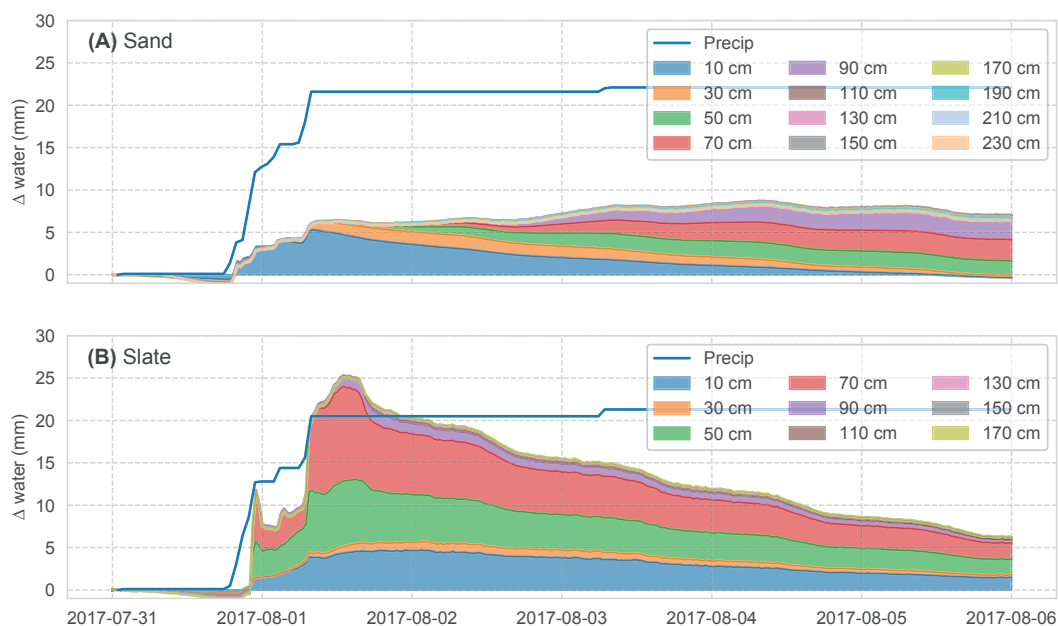
Figure 10. Event water balance observed at both sites. Change of soil water content in each colour-coded reference depth layer. Cumulated above-canopy precipitation input given as blue line.

the sites. At the sandy site, the fraction of the precipitation which is not intercepted in the canopy and litter layer enters the top soil horizon and successively percolates through the soil profile. The overall event water balance remains constant. At the slate site, the same event causes a fast response in deeper soil layers with an initially quick recession of the free water. This is followed by a diffusive redistribution into the surrounding soil aggregates seen as parallel declines of soil moisture in the

5   different depth layers.

In conclusion, the sandy site follows the expected event reaction of an ideal porous medium (Figure 10A). The assumption that the rhizosphere soil water dynamics is represented in our profile appears well-justified, and the roots will most likely source water from the soil matrix.

At the slate site, the hydrological regime is dominated by flashy transport through the macroporous soils and fill-and-spill

10   mechanisms of subsurface pools on the fissured bedrock (Figure 10B). Since soil moisture is measured as bulk apparent dielectric permittivity, the measurement principle has to integrate over the total sensed volume, irrespectively of stone fraction, voids or wetted contact surfaces. Here, roots are likely to grow along joints and fractures, where event-water can be stored with little effect on the bulk soil moisture. As such, the measurements might miss parts of the active rhizosphere.

4.4   Dynamic sourcing of RWU

15   The sourcing of RWU from different depths and the respective matric potential allows an alternative view of the data by relating RWU to soil state and depth (Fig. 11). Although no clear correlation of RWU and matric potential can be seen, the depth-related
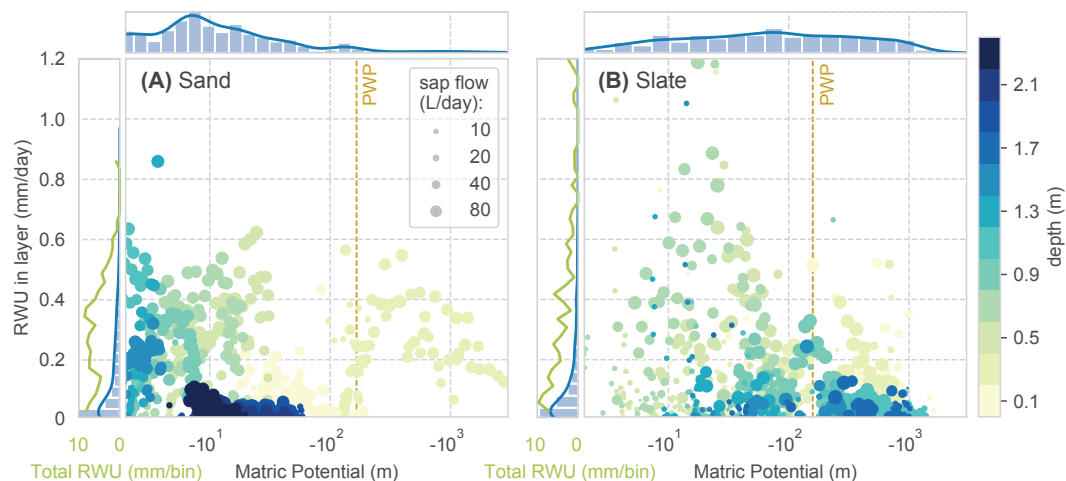
Figure 11. Sourcing of RWU: Daily values of matric potential in each soil layer and RWU. Colour coding with respective depth. Dot size marks the reference sap flow of the day. The marginal histograms and kernel density distributions on top refer to the occurrence of the respective matric potential bin in the observed period. The marginals on the left give the distribution of RWU (blue) and the total RWU of a certain bin (green). PWP marks a matric potential at the wilting point with pF 4.2.

colour coding corroborates the strong differences between the sites. In general, there is more tolerance of RWU to higher matric potential at the sand site. Given the slight tendency to higher maximal rates at lower matric potential above the wilting point (PWP), the high RWU rates at higher tensions might point to limits in the simplistic retention function application. The less bound water in deeper layers appears not to contribute much to RWU. In the slate regosol the pattern is more diverse but also more intuitive. Highest RWU rates occur at relatively low matric potential in moderate depths. However, high observed sap flows (large dots) also coincide with high matric potential and reactions in various depths. At the sand site, a correlation of matric potential and depth appears to exist, which is in line with the observed event reaction (Fig. 10).

5   Discussion

Our results give an ambivalent picture: Inferring RWU from changes in soil moisture within the rhizosphere was possible with our approach and provides interesting insights into the hydrological functioning of the root system for individual sites. The relatively high temporal resolution and spatial distribution of the data enabled a perspective into the rhizosphere water dynamics which is often conceptualised in models (Kuhlmann et al., 2012) but rarely measured. At the same time, we pointed out considerable limitations to the approach with respect to soil water state (no detectable signal during low moisture periods) and soil properties (high variability in heterogeneous soil profiles).
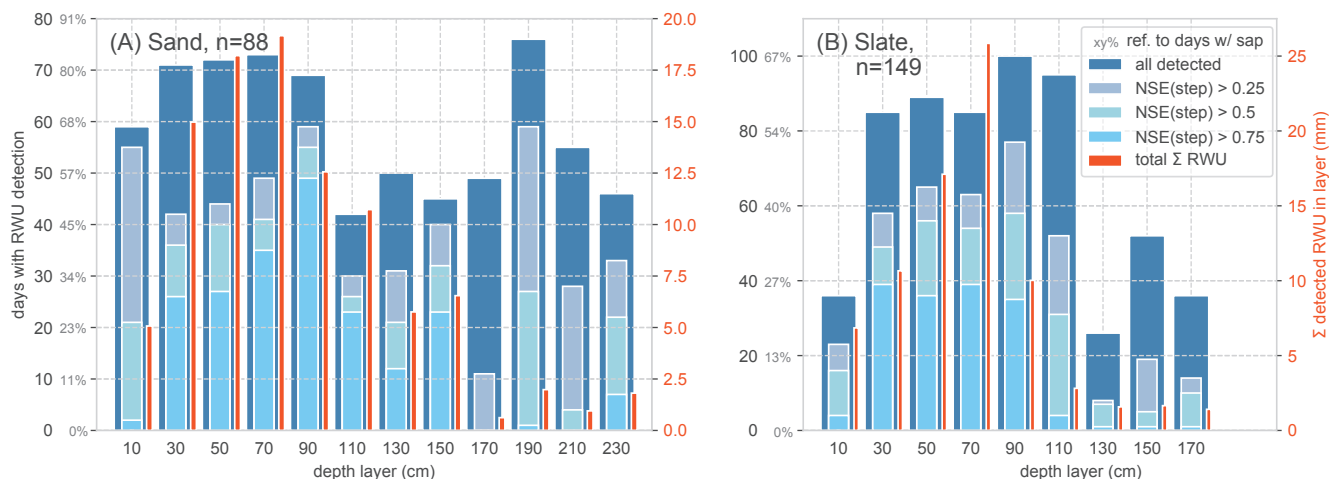
Figure 12. Number of detected days with RWU (blue) and the total sum of RWU over the season (red) for each depth layer. The compliance with the hypothesised step shape is days exceeding a given NSE. Reference number (n) refers to days with a total sap flow above $100\,\mathrm{mL}$. To this reference the percentage of days is given.

5.1 Performance of the RWU derivation function

The RWU derivation function appears to perform very well in general and can be used to evaluate a broad range of diurnal changes in soil moisture (Fig. 12). In the most active part of the rhizosphere (between $0.2\,\mathrm{m}$ and $1\,\mathrm{m}$, Fig. 12) at the sandy site, RWU was detected in about 80% of days with sap flow larger than $100\,\mathrm{mL}$. A large proportion of steps could be identified with

5 acceptable certainty (high NSE of step-shape as in Fig. 4B, see also Fig. C1). At the slate site about 60% of SF days are also found with RWU in the most active part of the rhizosphere. Unlike the first impression in Fig. 6, the proportion of steps with higher uncertainty about the actual fit of the shape with the assumptions is higher in the slate site data, which is in line with the lower overall RWU detection there.

The analyses of the temporal dynamics and the differences between the two sites (Fig. 8) hint at conceptual limits of our

10 approach and experimental design: Under somewhat ideal conditions with soil moisture sensors and roots in good contact with a rather homogeneous soil matrix and sufficient soil water availability, the diurnal steps are identified and evaluated with great confidence. In the regosol with high gravel content at the slate site, the approach is challenged when roots may source water from local pools, at contact interfaces with rocks, or in the periglacial cover beds. The high sap velocity despite higher matric tension in the soil might be actually supplied from regions outside the monitored soil moisture profile. Although the depth

15 resolution is very insightful, the likely non-homogeneous rhizosphere might not be fully represented by a single soil moisture profile and neglecting lateral differences. Effects such as highly active fine roots at the newly growing root tips might be overlooked. Additionally, we greatly simplified the complex form and function of the tree root architecture (Pregitzer, 2008) in

the assumption of a cylindrical, evenly utilised rhizosphere. However, we hope to have contributed an utilisable implementation for further applications (Jackisch, 2019) extending the works of Feddes and van Dam (2005); Guderle and Hildebrandt (2015).

5.2 Correlation of RWU and SF

Advancing means to monitor soil-water-plant dynamics is one of the overarching aims of this study. Given the generally

5   acceptable degree of correlation between soil moisture-derived RWU and sap flow (Fig. 7), one might be tempted to consider both measurements interchangeable for estimating transpiration. The analysis of the temporal development of their correlation (Fig. 8) contradicts this notion. We thus argue that observing the plant system at different gauges (RWU, SF, stem storage, leaf-level transpiration) provides the chance to actually analyse the underlying processes. This might help to answer the questions: Why is there a shift of the regression between RWU and SF over time? What is the optimisation function of the plant's RWU

10   sourcing (e.g. Gao et al., 2014) and SF variability (Saveyn et al., 2008)?

    Moreover, not only the presented RWU derivation has uncertainty. Measuring sap flow is influenced by response of the plant to wounding by the sensor installation, and by non-homogeneous xylem depths and associated differences in water transport around the stem (e.g. Bieker and Rust, 2010). The correlation between RWU inferred from soil moisture dynamics and SF appears to be an interesting means for further studies of plant dynamics in adaptation to environmental conditions. Since

15   our working-hypothesis of an instantaneously closed water balance between RWU and SF could not be corroborated, further studies could benefit from measuring RWU and SF complementarily in order to gain more knowledge on the various influences and temporal dynamics of this correlation.

5.3 Effects of the sites and controls for RWU

Despite very similar sap flow signals, the two sites have quite different RWU patterns (Fig. 9). It is interesting to note that the

20   main differences in RWU occur during the leaf-out phase until end of June. SF at the two sites is highly similar throughout the year. Thus, very different subsurface water states and sources result in similar fluxes in the trees. It is not a new hypothesis that trees optimise their water supply in the process of photosynthesis (Schymanski et al., 2008). The presented measurements may be a means to complement analyses of the links between subsurface and stand organisation (Metzger et al., 2017) and transpiration of trees (Renner et al., 2016).

25   However, the third hypothesis that the tension gradient controls RWU, cannot be clearly answered in this experiment and demands further research. Generally, the idea that the tree would minimise its cost for water (by sourcing large sap flows through RWU from layers with low matric potential) does not appear to be the full story (this would mean large light coloured dots at low matric potential and high RWU in Fig. 11). At the sandy site, only low RWU rates could be identified in the wet but deep layers. The correlation of matric potential with depth is apparent. However, all depth layers and soil water states almost

30   equally contributed to RWU. At the slate site, there appears a peak in RWU from intermediate depth (around $0.7\,\mathrm{m}$) and low matric potential. Despite the deeper layers clustering at higher tensions, lower RWU rates and higher SF, the sourcing of RWU is not easily reducible to a first-order relationship. High SF and moderate RWU against matric potentials higher than the wilting point might be explained with sources not captured by the soil moisture measurements (deeper pools or local stores).

Given this finding, the conceptualisation of plant-soil-water relations as capillary concept (e.g. Janott et al., 2010) might have essential limits with respect to analyses under changing conditions. With respect to multiple functions and specialisations of different roots in the root system (Kerk and Sussex, 2001), the controls of RWU and resulting transpiration require more specific approaches with higher spatiotemporal resolution. This is also the case for hydraulic redistribution in the rhizosphere

5 (Neumann and Cardon, 2012), which we neglected as minor effect in this study.

5.4 Outlook

As we have shown for moderately moist conditions, an estimate of RWU appears reasonably robust. Applications of RWU studies based on changes in soil moisture might benefit from laterally distributed or spatially continuous monitoring. Adding this to SF measurements gauging different roots (Lott et al., 1996) and analyses of stable isotope concentration in the xylem

10 water (Rothfuss and Javaux, 2017) could avoid overly simplistic assumptions about soil water availability and mixing. Analyses with higher temporal resolution could also elucidate further details about diurnal variations in xylem water isotopic signatures (De Deurwaerder et al., 2019). Moreover, higher spatial coverage and resolution using hydrogeophysical, quantitative measurements like time-lapse ground penetrating radar (Allroggen et al., 2017; Jackisch et al., 2017) would enable further analyses of the active rhizosphere and its geometry. With quantitative data about root zone soil moisture dynamics, cosmic ray measure-

15 ments could be a means to cover larger spatial scales (Nguyen et al., 2019). Eventually, a more realistic implementation of all compartments controlling transpiration into land surface models (e.g. Kennedy et al., 2019) could support analyses of stressors and adaptability under shifting environmental conditions.

6 Conclusions

Inferring RWU from changes in soil moisture during days without percolation is promising. An automated evaluation of

20 respective time series of soil water state dynamics over a profile within the rhizosphere can be conveniently applied. However, the approach is not universally suitable. The more complex the pedological setting, the more uncertain the estimate becomes. High precision and low noise in soil moisture measurements are a prerequisite for the method, especially when using an automated detection of the diurnal soil moisture decline. Furthermore, monitoring the whole rhizosphere profile instead of preselected depths proved important because the sourcing of the transpiration signal changes over the year.

25 Our study shows that RWU and sap flow cannot be used interchangeably as estimates for transpiration. In fact they give complementary information to understand the whole process from the soil water sourcing, transport through the tree towards eventual transpiration to the atmosphere. At our sites, we observed very different patterns in RWU despite similar sap flow and almost identical atmospheric forcing. However, contrary to the theoretical assumption for many transpiration models, soil matric potential appears not to be the only control.

30 Transpiration in forests is influenced by both site conditions and plant characteristics and their site adaptations. Therefore an experimental design of field studies measuring the different aspects of transpiration complementarily is promising (e.g.
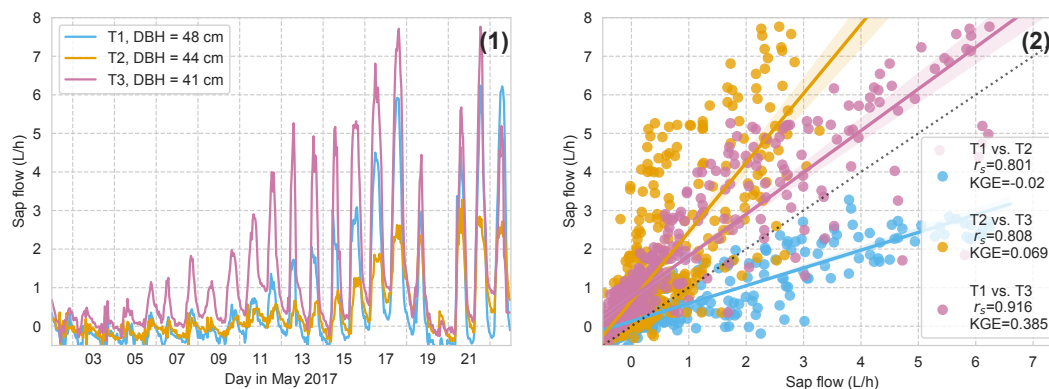
Figure A1. Hourly sap flow of all three beech trees at the slate site. (1) Time series, (2) Correlation between time series. T3 is the tree at the soil moisture profile. T1 is the tree used as reference in the study.

RWU from different profiles within the rhizosphere, sap flow, stem storage and leaf-level transpiration) to gain a holistic understanding of transpiration.

Code and data availability. The used RWU and sap flow calculation toolbox is published as Python package on GitHub (Jackisch, 2019). The data is available via GFZ Data Services (Jackisch and Hassler, 2019).

5 Appendix A: Slate site sap flow reference

At the slate site, the sap velocity measurement in the intended tree for reference failed three weeks after leaf-out (T3, DBH of $41\,cm$). Hence we needed to refer to another beech tree at the site (T1, DBH of $48\,cm$). The correlation of sap flow of all three monitored beech trees at the site (Figure A1) shows convincing overall signal similarity (r_s>0.8) but stronger deviation in absolute sap flow values (low KGE). Please note that the three weeks after leaf-out also showed the strongest deviation

10 between the sap flow of the two sites (Figure 9 1 & 2). We selected the tree no. 1 to replace the intended tree no. 3 as reference based on the best correlation measures.

Appendix B: Soil retention parameters

In the following a table of the site soil properties as van Genuchten parameters is given (Table A1).

	Sand (5-30 cm)	Sand (30-70 cm)	Slate (5-30 cm)	Slate (30-70 cm)
θ_{sat}	0.46	0.49	0.535	0.517
θ_{res}	0.041	0.041	0.011	0.028
α	0.84	1.71	4.13	4.39
n	1.47	1.64	1.21	1.21
m	0.32	0.39	0.17	0.17
k_{sat}	7.4e-5	6.5e-5	1.92e-4	4.13e-4

Table A1. Table of measured soil water retention curve parameters. θ in $\mathrm{m^3\,m^{-3}}$, α in $\mathrm{m^{-1}}$, k_{sat} in $\mathrm{m\,s^{-1}}$
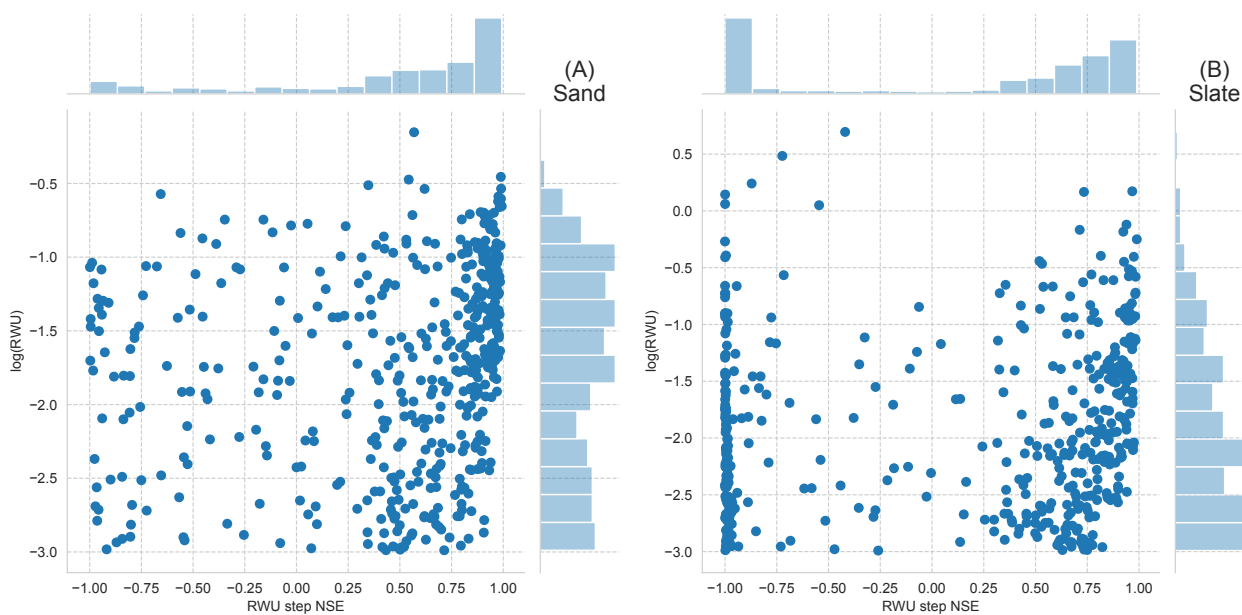

Figure C1. Identified RWU (log10 of RWU in mm/day on y-axes) and corresponding step coherence as NSE of synthetic step (x-axes) for the sandy site (A) and slate site (B). Marginals give respective histograms.

Appendix B: Uncertainty of RWU calculation

We report further details about the identified RWU and the respective NSE of the step-shape (Figure C1). With low correlation at all values for RWU, there is no indication for a detection threshold. At the slate site, a larger number of days have a NSE below zero, which might be false-positive results but which might also be another manifestation of the site characteristics discussed earlier.

Biogeosciences Open Access
Discussions

EGU

Author contributions. .

CJ and SH developed the study layout, performed the field work, prepared the data and composed the manuscript. SK did the first analyses on this data for his BSc thesis. CJ developed the detection algorithm, compiled most of the data analysis and plots with frequent discussion with SH. TB did preliminary RWU analyses based on soil moisture dynamics within the CAOS
5   research unit. The resulting discussions between TB, EZ, SH and CJ initially triggered the study. EZ and TB supportively accompanied the study and contributed during the manuscript preparation.

Competing interests. The authors declare no competing interests.

Biogeosciences
Discussions

Open Access
EGU

References

Allroggen, N., Jackisch, C., and Tronicke, J.: Four-dimensional gridding of time-lapse GPR data, in: 2017 9th International Workshop on Advanced Ground Penetrating Radar (IWAGPR), pp. 1–4, IEEE, https://doi.org/10.1109/IWAGPR.2017.7996067, https://doi.org/10.1109/IWAGPR.2017.7996067, 2017.

5 Bieker, D. and Rust, S.: Non-Destructive Estimation of Sapwood and Heartwood Width in Scots Pine (Pinus sylvestris L.), Silva Fennica, 44, 267–273, 2010.

Blume, T., Heidbüchel, I., Simard, S., Güntner, A., and Weiler, M.: Detecting spatio-temporal controls on depth distributions of root water uptake using soil moisture patterns, in: EGU General Assembly Conference Abstracts, pp. EPSC2016–16 444, https://meetingorganizer.copernicus.org/EGU2016/EGU2016-16444.pdf, 2016.

10 Blume, T., Hassler, S. K., and Weiler, M.: From groundwater to soil moisture to transpiration: do stable landscape patterns exist and when do they break down?, in: EGU General Assembly 2018, Vienna, https://meetingorganizer.copernicus.org/EGU2018/EGU2018-12735.pdf, 2018.

Boaga, J., Rossi, M., and Cassiani, G.: Monitoring Soil-plant Interactions in an Apple Orchard Using 3D Electrical Resistivity Tomography, Procedia Environmental Sciences, 19, 394–402, http://www.sciencedirect.com/science/article/pii/S1878029613003150, 2013.

15 Burgess, S. S. O., Adams, M. A., TURNER, N. C., and Ong, C. K.: The redistribution of soil water by tree root systems, Oecologia, 115, 306–311, https://doi.org/10.1007/s004420050521, https://link.springer.com/article/10.1007/s004420050521, 1998.

Burgess, S. S. O., Adams, M. A., and Bleby, T. M.: Measurement of sap flow in roots of woody plants: a commentary, Tree Physiology, 20, 909–913, https://doi.org/10.1093/treephys/20.13.909","keywords":["heat, https://doi.org/10.1093/treephys/20.13.909, 2000.

Cai, G., Vanderborght, J., Langensiepen, M., Schnepf, A., Hüging, H., and Vereecken, H.: Root growth, water uptake, and sap flow of winter
20 wheat in response to different soil water conditions, Hydrology and Earth System Sciences, 22, 2449–2470, https://doi.org/10.5194/hess-22-2449-2018, https://www.hydrol-earth-syst-sci.net/22/2449/2018/, 2018.

Carminati, A., Vetterlein, D., Koebernick, N., Blaser, S., Weller, U., and Vogel, H.-J.: Do roots mind the gap?, PLANT AND SOIL, 367, 651–661, https://doi.org/10.1007/s11104-012-1496-9, https://link.springer.com/article/10.1007/s11104-012-1496-9, 2012.

Carminati, A., Zarebanadkouki, M., Kroener, E., Ahmed, M. A., and Holz, M.: Biophysical rhizosphere processes affecting root water uptake,
25 Ann Bot, 118, 561–571, https://doi.org/10.1093/aob/mcw113","keywords":["Hydraulic, https://doi.org/10.1093/aob/mcw113, 2016.

Čermák, J., Kučera, J., and Nadezhdina, N.: Sap flow measurements with some thermodynamic methods, flow integration within trees and scaling up from sample trees to entire forest stands, Trees, 18, 529–546, https://doi.org/10.1007/s00468-004-0339-6, https://link.springer.com/article/10.1007/s00468-004-0339-6, 2004.

Couvreur, V., Vanderborght, J., and Javaux, M.: A simple three-dimensional macroscopic root water uptake model based on the hydraulic
30 architecture approach, Hydrology and Earth System Sciences, 16, 2957–2971, https://doi.org/10.5194/hess-16-2957-2012, https://www.hydrol-earth-syst-sci.net/16/2957/2012/, 2012.

De Deurwaerder, H., Visser, M. D., Detto, M., Boeckx, P., Meunier, F., Zhao, L., Wang, L., and Verbeeck, H.: Diurnal variation in xylem water isotopic signature biases depth of root-water uptake estimates, bioRxiv, 103, 712 554, https://doi.org/10.1101/712554, http://biorxiv.org/lookup/doi/10.1101/712554, 2019.

35 Dubbert, M. and Werner, C.: Water fluxes mediated by vegetation: emerging isotopic insights at the soil and atmosphere interfaces., The New phytologist, 221, 1754–1763, https://doi.org/10.1111/nph.15547, https://onlinelibrary.wiley.com/doi/abs/10.1111/nph.15547, 2019.

Feddes, R. A. and van Dam, J. C.: PLANT–SOIL–WATER RELATIONS, in: Encyclopedia of Soils in the Environment, edited by Hillel, D., pp. 222–230, Elsevier, Oxford, http://www.sciencedirect.com/science/article/pii/B0123485304005208, 2005.

Gao, H., Hrachowitz, M., Schymanski, S. J., Fenicia, F., Sriwongsitanon, N., and Savenije, H. H. G.: Climate controls how ecosystems size the root zone storage capacity at catchment scale, Geophysical Research Letters, 41, 2014GL061 668–7923, https://doi.org/10.1002/2014GL061668, http://dx.doi.org/10.1002/2014GL061668, 2014.

Gebauer, T., Horna, V., and Leuschner, C.: Variability in radial sap flux density patterns and sapwood area among seven co-occurring temperate broad-leaved tree species., Tree Physiology, 28, 1821–1830, https://doi.org/10.1093/treephys/28.12.1821, https://academic.oup.com/treephys/article-lookup/doi/10.1093/treephys/28.12.1821, 2008.

Gebler, S., Hendricks Franssen, H. J., Pütz, T., Post, H., Schmidt, M., and Vereecken, H.: Actual evapotranspiration and precipitation measured by lysimeters: a comparison with eddy covariance and tipping bucket, Hydrology and Earth System Sciences, 19, 2145–2161, https://doi.org/10.5194/hess-19-2145-2015, http://www.hydrol-earth-syst-sci.net/19/2145/2015/, 2015.

Guderle, M. and Hildebrandt, A.: Using measured soil water contents to estimate evapotranspiration and root water uptake profiles – a comparative study, Hydrology and Earth System Sciences, 19, 409–425, https://doi.org/10.5194/hess-19-409-2015-supplement, www.hydrol-earth-syst-sci.net/19/409/2015/, 2015.

Guderle, M., Bachmann, D., Milcu, A., Gockele, A., Bechmann, M., Fischer, C., Roscher, C., Landais, D., Ravel, O., Devidal, S., Roy, J., Gessler, A., Buchmann, N., Weigelt, A., and Hildebrandt, A.: Dynamic niche partitioning in root water uptake facilitates efficient water use in more diverse grassland plant communities, Functional Ecology, 32, 214–227, https://doi.org/10.1111/1365-2435.12948, https://besjournals.onlinelibrary.wiley.com/doi/full/10.1111/1365-2435.12948, 2018.

Hassler, S. K., Weiler, M., and Blume, T.: Tree-, stand- and site-specific controls on landscape-scale patterns of transpiration, Hydrology and Earth System Sciences, 22, 13–30, https://doi.org/10.5194/hess-22-13-2018, https://www.hydrol-earth-syst-sci.net/22/13/2018/, 2018.

Hildebrandt, A., Kleidon, A., and Bechmann, M.: A thermodynamic formulation of root water uptake, Hydrology and Earth System Sciences, 20, 3441–3454, https://doi.org/10.5194/hess-20-3441-2016-supplement, http://www.hydrol-earth-syst-sci.net/20/3441/2016/hess-20-3441-2016-supplement.pdf, 2016.

Jackisch, C.: Linking structure and functioning of hydrological systems - How to achieve necessary experimental and model complexity with adequate effort, Ph.D. thesis, KIT Karlsruhe Institute of Technology, Karlsruhe, https://doi.org/10.5445/IR/1000051494, 2015.

Jackisch, C.: Rootwater Python Package: Initial release, MIT license, https://doi.org/10.5281/zenodo.3556433, available at https://github.com/cojacoo/rootwater, 2019.

Jackisch, C. and Hassler, S. K.: Rhizosphere soil moisture dynamics and sap flow – determining root water uptake in a case study in the Attert catchment in Luxembourg, GFZ Data Services, https://doi.org/10.5880/fidgeo.2019.030, http://pmd.gfz-potsdam.de/panmetaworks/review/2d59f8dd57898ba031d134d795a0bd38a0e7849469238567dad5a14945ef975b/, 2019.

Jackisch, C., Angermann, L., Allroggen, N., Sprenger, M., Blume, T., Tronicke, J., and Zehe, E.: Form and function in hillslope hydrology: in situ imaging and characterization of flow-relevant structures, Hydrology and Earth System Sciences, 21, 3749–3775, https://doi.org/10.5194/hess-21-3749-2017, https://www.hydrol-earth-syst-sci.net/21/3749/2017/, 2017.

Janott, M., Gayler, S., Gessler, A., Javaux, M., Klier, C., and Priesack, E.: A one-dimensional model of water flow in soil-plant systems based on plant architecture, PLANT AND SOIL, 341, 233–256, https://doi.org/10.1007/s11104-010-0639-0, https://link.springer.com/article/10.1007/s11104-010-0639-0, 2010.

Jasechko, S., Sharp, Z. D., Gibson, J. J., Birks, S. J., Yi, Y., and Fawcett, P. J.: Terrestrial water fluxes dominated by transpiration., Nature, 496, 347–350, https://doi.org/10.1038/nature11983, http://www.nature.com/articles/nature11983, 2013.

Javaux, M., Schröder, T., Vanderborght, J., and Vereecken, H.: Use of a Three-Dimensional Detailed Modeling Approach for Predicting Root Water Uptake, VADOSE ZONE JOURNAL, 7, 1079–1088, https://doi.org/10.2136/vzj2007.0115, https://www.soils.org/publications/vzj/abstracts/7/3/1079, 2008.

Kennedy, D., Swenson, S., Oleson, K. W., Lawrence, D. M., Fisher, R., da Costa, A. C. L., and Gentine, P.: Implementing
5   Plant Hydraulics in the Community Land Model, Version 5, Journal of Advances in Modeling Earth Systems, 11, 485–513, https://doi.org/10.1029/2018MS001500, https://agupubs.onlinelibrary.wiley.com/doi/full/10.1029/2018MS001500, 2019.

Kennedy, S.: Astral, https://github.com/sffjunkie/astral, 2019.

Kerk, N. M. and Sussex, I. M.: Roots and Root Systems, vol. 448, American Cancer Society, Chichester, UK, 3 edn., https://doi.org/10.1002/9780470015902.a0002058.pub2, https://onlinelibrary.wiley.com/doi/full/10.1002/9780470015902.a0002058.
10   pub2, 2001.

Klenk, P., Jaumann, S., and Roth, K.: Quantitative high-resolution observations of soil water dynamics in a complicated architecture using time-lapse ground-penetrating radar, Hydrology and Earth System Sciences, 19, 1125–1139, https://doi.org/10.5194/hess-19-1125-2015, http://www.hydrol-earth-syst-sci.net/19/1125/2015/hess-19-1125-2015-supplement.zip, 2015.

Kroener, E., Holz, M., Zarebanadkouki, M., Ahmed, M., and Carminati, A.: Effects of Mucilage on Rhizosphere Hydraulic Functions
15   Depend on Soil Particle Size, VADOSE ZONE JOURNAL, 17, 0, https://doi.org/10.2136/vzj2017.03.0056, https://dl.sciencesocieties.org/publications/vzj/abstracts/17/1/170056, 2018.

Kuhlmann, A., Neuweiler, I., van der Zee, S. E. A. T. M., and Helmig, R.: Influence of soil structure and root water uptake strategy on unsaturated flow in heterogeneous media, Water Resources Research, 48, https://doi.org/10.1029/2011WR010651, http://gateway.webofknowledge.com/gateway/Gateway.cgi?GWVersion=2&SrcAuth=mekentosj&SrcApp=Papers&DestLinkType=
20   FullRecord&DestApp=WOS&KeyUT=000301133200002, 2012.

Leuschner, C., Coners, H., and Icke, R.: In situ measurement of water absorption by fine roots of three temperate trees: species differences and differential activity of superficial and deep roots., Tree Physiology, 24, 1359–1367, http://eutils.ncbi.nlm.nih.gov/entrez/eutils/elink.fcgi?dbfrom=pubmed&id=15465698&retmode=ref&cmd=prlinks, 2004.

Loritz, R., Hassler, S. K., Jackisch, C., Allroggen, N., Schaik, L. V., Wienhöfer, J., and Zehe, E.: Picturing and modeling catchments by
25   representative hillslopes, Hydrology and Earth System Sciences, 21, 1225–1249, https://doi.org/10.5194/hess-21-1225-2017, https://www.hydrol-earth-syst-sci.net/21/1225/2017/, 2017.

Lott, J. E., Khan, A. A. H., Ong, C. K., and Black, C. R.: Sap flow measurements of lateral tree roots in agroforestry systems., Tree Physiology, 16, 995–1001, https://doi.org/10.1093/treephys/16.11-12.995, https://academic.oup.com/treephys/article-lookup/doi/10.1093/treephys/16.11-12.995, 1996.

30   Mary, B., Saracco, G., Peyras, L., Vennetier, M., Mériaux, P., and Camerlynck, C.: Mapping tree root system in dikes using induced polarization: Focus on the influence of soil water content, Journal of Applied Geophysics, 135, 387–396, https://doi.org/10.1016/j.jappgeo.2016.05.005, https://linkinghub.elsevier.com/retrieve/pii/S0926985116301331, 2016.

Maxwell, R. M. and Condon, L. E.: Connections between groundwater flow and transpiration partitioning., SCIENCE, 353, 377–380, https://doi.org/10.1126/science.aaf7891, http://www.sciencemag.org/cgi/doi/10.1126/science.aaf7891, 2016.

35   Metzger, J. C., Wutzler, T., Valle, N. D., Filipzik, J., Grauer, C., Lehmann, R., Roggenbuck, M., Schelhorn, D., Weckmüller, J., Küsel, K., Totsche, K. U., Trumbore, S., and Hildebrandt, A.: Vegetation impacts soil water content patterns by shaping canopy water fluxes and soil properties, 31, 3783–3795, https://doi.org/10.1002/hyp.11274, https://onlinelibrary.wiley.com/doi/full/10.1002/hyp.11274, 2017.

Nadezhdina, N., David, T. S., David, J. S., Ferreira, M. I., Dohnal, M., Tesar, M., Gartner, K., Leitgeb, E., Nadezhdin, V., Cermak, J., Jimenez, M. S., and Morales, D.: Trees never rest: the multiple facets of hydraulic redistribution, Ecohydrology, 3, 431–444, https://doi.org/10.1002/eco.148, http://dx.doi.org/10.1002/eco.148, 2010.

Neumann, R. B. and Cardon, Z. G.: The magnitude of hydraulic redistribution by plant roots: a review and synthesis of empirical and modeling studies., The New phytologist, 194, 337–352, https://doi.org/10.1111/j.1469-8137.2012.04088.x, http://doi.wiley.com/10.1111/j.1469-8137.2012.04088.x, 2012.

Neuper, M. and Ehret, U.: Quantitative precipitation estimation with weather radar using a data-and information-based approach, hydrol-earth-syst-sci-discuss.net, https://www.hydrol-earth-syst-sci-discuss.net/hess-2018-606/hess-2018-606.pdf, 2019.

Nguyen, H. H., Jeong, J., and Choi, M.: Extension of cosmic-ray neutron probe measurement depth for improving field scale root-zone soil moisture estimation by coupling with representative in-situ sensors, Journal of Hydrology, 571, 679–696, https://linkinghub.elsevier.com/retrieve/pii/S0022169419301751, 2019.

Oki, T. and Kanae, S.: Global Hydrological Cycles and World Water Resources, SCIENCE, 313, 1068–1072, https://doi.org/10.1126/science.1128845, http://www.sciencemag.org/cgi/doi/10.1126/science.1128845, 2006.

Or, D., Lehmann, P., Shahraeeni, E., and Shokri, N.: Advances in Soil Evaporation Physics—A Review, VADOSE ZONE JOURNAL, 12, 0, https://doi.org/10.2136/vzj2012.0163, https://www.soils.org/publications/vzj/abstracts/12/4/vzj2012.0163, 2013.

Pagès, L., Vercambre, G., Drouet, J.-L., Lecompte, F., Collet, C., and Le Bot, J.: Root Typ: a generic model to depict and analyse the root system architecture, PLANT AND SOIL, 258, 103–119, https://doi.org/10.1023/B:PLSO.0000016540.47134.03, https://doi.org/10.1023/B:PLSO.0000016540.47134.03, 2004.

Pfister, L., Trebs, I., Hoffmann, L., Iffly, J. F., Matgen, P., Tailliez, C., Schoder, R., Lepesant, P., Frisch, C., Kipgen, R., Göhlhausen, D., Ernster, R., and Schleich, G.: Atlas hydro-climatologique du Grand-Duché de Luxembourg, Tech. rep., 2014.

Pohlmeier, S. H., Vanderborght, J., and Pohlmeier, A.: Quantitative mapping of solute accumulation in a soil-root system by magnetic resonance imaging, Water Resources Research, 53, 7469–7480, https://doi.org/10.1002/2017WR020832, https://agupubs.onlinelibrary.wiley.com/doi/full/10.1002/2017WR020832, 2017.

Poyatos, R., Granda, V., Molowny-Horas, R., Mencuccini, M., Steppe, K., and Martínez-Vilalta, J.: SAPFLUXNET: towards a global database of sap flow measurements, Tree Physiology, 36, 1449–1455, https://doi.org/10.1093/treephys/tpw110, https://academic.oup.com/treephys/article-lookup/doi/10.1093/treephys/tpw110, 2016.

Pregitzer, K. S.: Tree root architecture–form and function., The New phytologist, 180, 562–564, https://doi.org/10.1111/j.1469-8137.2008.02648.x, http://doi.wiley.com/10.1111/j.1469-8137.2008.02648.x, 2008.

Renner, M., Hassler, S. K., Blume, T., Weiler, M., Hildebrandt, A., Guderle, M., Schymanski, S. J., and Kleidon, A.: Dominant controls of transpiration along a hillslope transect inferred from ecohydrological measurements and thermodynamic limits, Hydrology and Earth System Sciences, 20, 2063–2083, https://doi.org/10.5194/hess-20-2063-2016-supplement, http://www.hydrol-earth-syst-sci.net/20/2063/2016/hess-20-2063-2016-supplement.pdf, 2016.

Renner, M., Brenner, C., Mallick, K., Wizemann, H.-D., Conte, L., Trebs, I., Wei, J., Wulfmeyer, V., Schulz, K., and Kleidon, A.: Using phase lags to evaluate model biases in simulating the diurnal cycle of evapotranspiration: a case study in Luxembourg, Hydrology and Earth System Sciences, 23, 515–535, https://doi.org/10.5194/hess-23-515-2019, https://www.hydrol-earth-syst-sci.net/23/515/2019/, 2019.

Rodríguez-Robles, U., Arredondo, T., Huber-Sannwald, E., Ramos-Leal, J. A., and Yépez, E. A.: Technical note: Application of geophysical tools for tree root studies in forest ecosystems in complex soils, Biogeosciences, 14, 5343–5357, https://www.biogeosciences.net/14/5343/2017/bg-14-5343-2017.pdf, 2017.

Rössler, Günter: Rindenabzug richtig bemessen, Forstzeitung, 10, https://www.waldwissen.net/waldwirtschaft/holz/sortierung/bfw_rindenabzug/index_DE, 2008.

Rothfuss, Y. and Javaux, M.: Reviews and syntheses: Isotopic approaches to quantify root water uptake: a review and comparison of methods, BIOGEOSCIENCES, 14, 2199–2224, https://doi.org/10.5194/bg-14-2199-2017, https://www.biogeosciences.net/14/2199/2017/, 2017.

5 Saveyn, A., Steppe, K., and Lemeur, R.: Spatial variability of xylem sap flow in mature beech (Fagus sylvatica) and its diurnal dynamics in relation to microclimate, Botany, 86, 1440–1448, https://doi.org/10.1139/B08-112, http://www.nrcresearchpress.com/doi/10.1139/B08-112, 2008.

Schymanski, S., Sivapalan, M., Roderick, M., Hutley, L., and Beringer, J.: An optimality-based model of the dynamic feedbacks between natural vegetation and the water balance, Water Resources Research, 45, http://dx.doi.org/10.1029/2008WR006841, 2009.

10 Schymanski, S. J. and Or, D.: Leaf-scale experiments reveal an important omission in the Penman–Monteith equation, Hydrology and Earth System Sciences, 21, 685–706, https://doi.org/10.5194/hess-21-685-2017, http://www.hydrol-earth-syst-sci.net/21/685/2017/, 2017.

Schymanski, S. J., Roderick, M. L., Sivapalan, M., HUTLEY, L. B., and Beringer, J.: A canopy-scale test of the optimal water-use hypothesis, Plant, Cell and Environment, 31, 97–111, https://doi.org/10.1111/j.1365-3040.2007.01740.x, https://onlinelibrary.wiley.com/doi/full/10.1111/j.1365-3040.2007.01740.x, 2008.

15 Shuttleworth, W. J.: Putting the 'vap' into evaporation, Hydrology and Earth System Sciences, 11, 210–244, 2007.

Sperry, J. S. and Love, D. M.: What plant hydraulics can tell us about responses to climate-change droughts., The New phytologist, 207, 14–27, https://doi.org/10.1111/nph.13354, http://doi.wiley.com/10.1111/nph.13354, 2015.

Vidal, A., Hirte, J., Bender, S. F., Mayer, J., Gattinger, A., Höschen, C., Schädler, S., Iqbal, T. M., and Mueller, C. W.: Linking 3D Soil Structure and Plant-Microbe-Soil Carbon Transfer in the Rhizosphere, Frontiers in Environmental Science, 6, 36,

20 https://doi.org/10.3389/fenvs.2018.00009, http://journal.frontiersin.org/article/10.3389/fenvs.2018.00009/full, 2018.

Wrede, S., Fenicia, F., Martínez-Carreras, N., Juilleret, J., Hissler, C., Krein, A., Savenije, H. H. G., Uhlenbrook, S., Kavetski, D., and Pfister, L.: Towards more systematic perceptual model development: a case study using 3 Luxembourgish catchments, 29, 2731–2750, https://doi.org/10.1002/hyp.10393, http://doi.wiley.com/10.1002/hyp.10393, 2015.

Wulfmeyer, V., Turner, D. D., Baker, B., Banta, R., Behrendt, A., Bonin, T., Brewer, W. A., Buban, M., Choukulkar, A., Dumas, E., Hardesty,

25 R. M., Heus, T., Ingwersen, J., Lange, D., Lee, T. R., Metzendorf, S., Muppa, S. K., Meyers, T., Newsom, R., Osman, M., Raasch, S., Santanello, J., Senff, C., Späth, F., Wagner, T., Weckwerth, T., Turner, D. D., Baker, B., Banta, R., Behrendt, A., Bonin, T., Brewer, W. A., Buban, M., Choukulkar, A., Dumas, E., Hardesty, R. M., Heus, T., Ingwersen, J., Lange, D., Lee, T. R., Metzendorf, S., Muppa, S. K., Meyers, T., Newsom, R., Osman, M., Raasch, S., Santanello, J., Senff, C., Späth, F., Wagner, T., and Weckwerth, T.: A New Research Approach for Observing and Characterizing Land–Atmosphere Feedback, Bulletin of the American Meteorological Society,

30 https://doi.org/10.1175/BAMS-D-17-0009.1, https://journals.ametsoc.org/doi/abs/10.1175/BAMS-D-17-0009.1, 2018.

York, L. M., Carminati, A., Mooney, S. J., Ritz, K., and Bennett, M. J.: The holistic rhizosphere: integrating zones, processes, and semantics in the soil influenced by roots., Journal of Experimental Botany, 67, 3629–3643, https://doi.org/10.1093/jxb/erw108, https://academic.oup.com/jxb/article-lookup/doi/10.1093/jxb/erw108, 2016.